# Comparison between methods to estimate bicep femoris fascicle length from three estimation equations using a 10 cm ultrasound probe.

## Comparison between methods of estimating bicep femoris fascicle length.

**Abstract**

To aim of the present study was to determine the reliability and differences between three fascicle length (FL) estimation methods when utilising a 10 cm ultrasound (US) probe. Thirteen males (24.1±3.8years, 79.3±14kg, 179±6.6cm) participated. Bicep femoris long head ($BF_{LH}$) US images were collected on two separate occasions. Three previously established extrapolation methods were utilised. Near perfect reliability was observed for all methods. Criterion estimation resulted in a significant, trivial ($p$=0.016,$g$=0.17) increase in FL compared to the basic trigonometry equation with non-significant, trivial increase ($p$=0.081,$g$=0.10) between the criterion and partial measure method. The partial measure method was not significantly or meaningfully greater than the basic trigonometry method ($p$=0.286,$g$=0.08). Both alternative methods demonstrated unacceptable LOA (>5%), with hetroschedacity. All methods of extrapolation are reliable and could be used over time. However, as methods are not comparable, there could be a rationale to utilise underestimated results to ensure a degree of cushioning.

*Key words: Hamstring, fascicle length estimation, ultrasound, field of view.*

## Introduction

The complex architecture that makes up the biceps femoris long head ($BF_{LH}$) is potentially due to its diverse functioning (Koulouris & Connell, 2005). It is a biarticular muscle with multiple roles reported in both injury prevention and performance (Lieber & Ward, 2011), functioning as both a hip extensor and knee flexor (Morin et al., 2015; Schache et al., 2013). In the role of hamstring injury risk reduction, fascicle length (FL) of the $BF_{LH}$ may potentially have a large influence (Opar et al., 2012; Timmins et al., 2016a), impacting upon the muscle's force-velocity and force-length relationships (Timmins et al., 2016b). Due to the observed relationship between $BF_{LH}$ FL and hamstring strain injury (HSI) (Timmins et al., 2016; Timmins et al., 2015), measuring the $BF_{LH}$ fascicle via the use of ultrasound (US) has become common practice within elite sports (Ribeiro Alvares et al., 2019; Timmins et al., 2016a; Timmins et al., 2016b), with sport specific recommendations on $BF_{LH}$ FL, where the risk of HSI occurrence reduces (Timmins et al., 2016a). Within professional soccer, it has been reported that possessing a $BF_{LH}$ FL of < 10.56 cm increases the risk of sustaining a HSI 4.1-fold (Timmins et al., 2016a).

Currently, using ultrasound images alone, it is not possible to completely measure the entire length of the $BF_{LH}$ FL from a single image (Franchi et al., 2019); as the FLs generally exceed the field of view (FOV) of the probe (a typical probe length is 4 - 6 cm) (Behan et al., 2018; De Oliveira et al., 2016; Kellis et al., 2009; Pimenta et al., 2018; Timmins et al., 2016a; Timmins et al., 2015). As the whole fascicle is generally not in view within a single ultrasound image, it has traditionally been estimated via a combination of tangible architectural measurements and trigonometry. A criterion method of estimating FL (Equation 1), as proposed by Blazevich et al. (2006) and Kellis et al. (2009), includes measuring the aponeurosis angle (AA) (curvature of the deep aponeurosis in relation to the horizontal plane);

in addition to the pennation angle (PA) (angle of the fascicle relative to the deep aponeurosis) and muscle thickness (MT) (perpendicular distance between the deep and superficial aponeurosis) proceeding to use trigonometry calculations to estimate FL. A secondary method presented within the literature, originally proposed for assessment of the vastus lateralis by Guilhem and colleagues (2011), which has been used more recently to estimate $BF_{LH}$ FL (Franchi et al., 2019; Freitas et al., 2018; Pimenta et al., 2018), includes partially measuring a visible fascicle and estimating the smallest portion not within the field of view (FOV) (Equation 2). Previously researchers focusing on more symmetrical pennate muscle (vastus lateralis, triceps brachii) has utilised a third, more simplistic equation that does not consider the AA or any partial measure (Equation 3) (Kawakami et al., 1993). However, it would be hypothesized that methods which reduce the degree of estimation, via an increased single FOV or partial measure, could increase the accuracy and reliability of estimated measures of FL.

Previous research has demonstrated that all methods of $BF_{LH}$ FL estimation are highly reliable and can be used to routinely estimate $BF_{LH}$ FL (Franchi et al., 2019; Timmins et al., 2016a; Timmins et al., 2015). To the authors' knowledge, researchers that have compared FL estimation methods include ultrasonography estimation versus cadaver specimens (Kellis et al., 2009), in addition to a single image estimation versus an extended FOV image measurement (Franchi et al., 2019; Pimenta et al., 2018). All studies demonstrated that utilizing a single image estimation ($<6$ cm), significantly overestimated $BF_{LH}$ FL (Franchi et al., 2019; Kellis et al., 2009; Pimenta et al., 2018). With large percentage differences ($\geq$14.8%) from direct cadaver specimens (Kellis et al., 2009), and an approximately a 5-20% and overestimation bias between extended FOV and single image estimation equation depending on the estimation method utilised (Franchi et al., 2019; Pimenta et al., 2018). However, no study to date has compared between the methods of estimating $BF_{LH}$ FL when utilising a probe which enables an increased FOV. Therefore, the purpose of this study, was to determine the reliability of and conduct a comparison between three estimation methods (equation 1-3), when utilising a probe with a greater FOV (10 cm), than those previously reported. It was hypothesised that there would be non-significant differences between estimated FLs, as the large FOV (10 cm) enables the assessor to accurately identify the trajectory of specific fascicles within the $BF_{LH}$.

## Materials and Methods

### Experimental design

A test-retest observational design (Figure 1) was used to assess $BF_{LH}$ architectural parameters, including FL, across three equations derived from a large single probe with a large FOV (10 cm).

****INSERT FIGURE 1 ABOUT HERE****

Thirteen physically active males (age 24.1 ± 3.8 years, body mass 79.3 ± 14 kg, height 179 ± 6.6 cm) with no history of lower-limb injury or inflammatory conditions completed two testing sessions. All participants reported that they participated in team sports on a regular basis (soccer = 6, rugby = 4, futsal = 2 and American football = 1). Written informed consent was obtained from all participants prior to testing. The study was approved by the University of Salford institutional review board and conformed to the principles of the Declaration of Helsinki (1983).

Six images of the $BF_{LH}$ were captured with a 10 cm width ultrasound probe across two-sessions (three per session) within a 7-day period for both the left and right legs. One trained rater collected and digitized all images collected across both sessions. Between-session reliability was established across both time points.

## Procedures

### *Bicep Femoris Ultrasound Acquisition*

Initially the scanning site for all images was determined as the halfway point between the ischial tuberosity and the knee joint fold, along the line of the BF. Images were recorded while participants lay relaxed in a prone position, with the hip in neutral and the knee fully extended. Images were subsequently collected along the longitudinal axis of the muscle belly utilizing a 2D, B-mode ultrasound (MyLab 70 xVision, Esaote, Genoa, Italy) with a 7.5 MHz, 10 cm linear array probe with a depth resolution of 67 mm.

To collect the ultrasound images, a layer of conductive gel was placed across the linear array probe; the probe was then placed on the skin over the scanning site and aligned longitudinally to the BF and perpendicular to the skin. During collection of the ultrasound images, care was taken to ensure minimal pressure was applied to the skin, as a larger application of pressure distort images leading to temporarily elongated muscle fascicles. The assessor manipulated the orientation of the probe slightly if the superficial and intermediate aponeuroses were not parallel. These methods are consistent to those used previously (Timmins et al., 2016a; Timmins et al., 2015).

### *Bicep Femoris Architectural Digitization*

All sonograms were analysed off-line with Image J version 1.52 software (National Institute of Health, Bethesda, MD, USA). Images were first calibrated to the known length of the FOV, then for each image a fascicle of interest was identified. Finally, MT, PA, AA and observed

FL were measured three times within each image, to enable complete FL estimation. Three trigonometric linear equations were utilised within the present study:

$$FL = \sin(\mathrm{AA} + 90°)\ \mathrm{x}\ \mathrm{MT}/\sin(180° - (\mathrm{AA} + 180° - \mathrm{PA})$$

**Equation 1 Criterion fascicle length estimation equation** (Blazevich et al., 2006; Kellis et al., 2009)

$$FL = L + (h \div \sin(\beta))$$

**Equation 2 Fascicle length estimation partial measure equation, where L is the observable fascicle length, *h* is the perpendicular distance between the superficial aponeurosis and the fascicles visible endpoint and *β* is the angle between the fascicle and the superficial aponeurosis.** (Franchi et al., 2019; Freitas et al., 2018; Pimenta et al., 2018),

$$FL = MT/(\sin(PA))$$

**Equation 3 Fascicle length estimation basic trigonometry equation.** (Kawakami et al., 1993)

**Statistical Analyses**

Between-session reliability based on the mean of each architectural parameter for each session, was assessed via a series of two-way mixed effects intraclass correlation coefficients (ICCs), 95% confidence intervals (CI) and coefficient of variation (CV). A paired samples t-test and Hedge's $g$ effect sizes (ES) were utilized to determine if there were any significant differences between the session means. Minimum acceptable reliability was confirmed using a CV <10%. The ICC values will be interpreted as low (<0.30), moderate (0.30-0.49), high (0.50-0.69), very high (0.70-0.89), nearly perfect (0.90-0.99) and perfect (1.0). Standard error of measurement (SEM) was calculated using the formula; $(SD(Pooled) \times (\sqrt{1} - ICC)$, whereas the minimal detectable difference (MDD) was calculated from the formula; $\left((1.96 \times (\sqrt{2})\right) \times SEM)$. A repeated-measures analysis of variance (RMANOVA) and Bonferroni post hoc comparisons were conducted to determine if there were significant differences in the FL values between the different estimation methods. Hedge's $g$ ES and 95% CI were also calculated to determine the magnitude of differences using a custom excel spreadsheet.

The mean of the difference (bias) was expressed absolutely and as a percentage, ratio (criterion method/alternative method), 95% limits of agreement (LOA) (LOA: mean of the difference ± 1.96 standard deviations) and 95% CI were calculated between FL estimate methods using the methods described by Bland and Altman (1986). Unacceptable LOA were determined a priori as bias percentage greater than ±5%. Pearson's correlation coefficients and coefficient of determination ($R^2$) were used to determine the relationship between the three FL estimation methods. Correlations were interpreted using the scale described Hopkins (2002): trivial (<0.10), small (0.10-0.29), moderate (0.30-0.49), large (0.50-0.69), very large (0.7-0.89), nearly perfect (0.9-0.99), perfect (1).

Normality for all variables was confirmed using a Shapiro Wilks-test. Statistical significance was set at $P < 0.05$ for all tests. All Hedge's $g$ ES were interpreted as trivial (<0.19), small (0.20-0.59), moderate (0.60-1.19), large (1.20-1.99), and very large (≥2.0) (Hopkins, 2002).

**Results**

All data was normally distributed ($p > 0.05$). Near perfect between-session reliability was observed for all measures and estimation methods, with no significant (p>0.05) or meaningful

($d$ < 0.10) differences between testing sessions. The mean values, reliability statistics, SEM, MDD and observed percentages for $BF_{LH}$ architectural measurements are presented in Table 1.

****INSERT TABLE 1 ABOUT HERE****

****INSERT FIGURE 2 ABOUT HERE****

Mean FLs of 10.30-, 9.96- and 10.11 cm were observed for the criterion, basic trigonometry, and partial measure methods respectively (Figure 2). The criterion method resulting in a significantly ($p$ = 0.016) greater FL compared to the basic trigonometry method, although this was only trivial ($g$ [95% CI] = 0.17 [-0.58 to 0.93]). Non-significant and trivial differences ($p$ = 0.081, $g$ [95% CI] = 0.10 [-0.65 to 0.86]) were observed between the further measures, with the criterion measure being greater than the partial measure method, while the partial measure method was not significantly or meaningfully greater ($p$ = 0.286, $g$ [95% CI] = 0.08 [-0.68 to 0.84]) than the basic trigonometry method.

Both the basic trigonometry and partial measure methods demonstrated unacceptable LOA (Table 2) (>5%), when compared to the criterion measure. Individual Bland and Altman plots (Figure 3) illustrate heteroscedastic results between both methods in comparison to the criterion method.

****INSERT TABLE 2 ABOUT HERE****

****INSERT FIGURE 3 ABOUT HERE****

Despite almost perfect significant relationships observed between the basic trigonometry and partial measure method in comparison to the criterion estimation methods (Table 3, Figure 4), due to the heteroscedastic data, correction equations were not deemed to be applicable.

****INSERT TABLE 3 ABOUT HERE****

****INSERT FIGURE 4 ABOUT HERE****

## Discussion

The aim of this study was to observe the reliability of using the 10 cm probe, whilst also determining if any differences exist between the estimation methods. The three estimation methods all reached minimum acceptable and near perfect between-session reliability (Table 1). A significant, albeit trivial difference, was observed between the criterion and basic trigonometry methods, whereas non-significant and trivial differences were observed between all other measures. Between the criterion and both alternative methods an unacceptable degree of bias (LOA >5%) was observed, with very large and near perfect relationships. However, due to the heteroscedastic comparisons between the methods, it was not applicable for the development of correction equations.

For the $BF_{LH}$, both the criterion method and partial measurement method have previously demonstrated high ICCs, consistent with the present study: 0.79 – 0.98, 0.80- 0.99 and 0.85-0.96 for FL, MT and PA respectively (De Oliveira et al., 2016; Franchi et al., 2019; Freitas et al., 2018; Kellis et al., 2009; Pimenta et al., 2018; Timmins et al., 2015). The greater levels of reliability identified within the present study when compared to the previous research could be explained by a number of factors, firstly the inclusion of specific populations within previous research, including; women, non-trained males and cadaver specimens, could have all impacted upon the US image quality, potentially by an increase in subcutaneous and intramuscular adipose tissue as well as effect of mortality on muscle characteristics (De Oliveira et al., 2016; Freitas et al., 2018; Kellis et al., 2009; Pimenta et al., 2018). Secondly, the probe utilized within the present study had a field of view of 10 cm, this is in contrast to all previous work that has utilized shorter probes ~6 cm (De Oliveira et al., 2016; Franchi et al., 2019; Freitas et al., 2018; Kellis et al., 2009; Pimenta et al., 2018; Timmins et al., 2015). This greater FOV could have aided in image measurement accuracy and the resultant reliability of measurements, as more of the FL and surrounding structures (i.e. aponeuroses) to be imaged (Franchi et al., 2019), which is consistent within previous research comparing single image and extended FOV methods (Franchi et al., 2019). Although the larger 10 cm probe, used within the present study, has not been compared to its smaller counterparts within the literature.

Despite the observed minimal bias, there was an unacceptable LOA, with trivial differences identified and very large and near-perfect relationships identified between the estimation methods. Due to the heteroscedastic plots identified between methods, if correction equations were developed, they would have provided a poor ability to correct the resultant values. This could be a result of inconsistency of extrapolation methods, with subject specific over- or under-estimations affecting the observed bias (Franchi et al., 2019). Within the present study the mean $BF_{LH}$ FL measures estimated using basic trigonometry and partial measure methods underestimated $BF_{LH}$ FL in comparison to the criterion method although this was not consistent across all participants. This finding is supported by Franchi et al. (2019), who observed a similar overestimation when using the criterion method in comparison to the partial measure estimation methods. Although it should be noted that all methods of single image extrapolation, overestimate $BF_{LH}$ FL in comparison to all extended FOV methods (Franchi et al., 2019;

Pimenta et al., 2018), whereby the entire fascicle is imaged. This would indicate that extended FOV methods are a superior imaging technique, however, extended FOV methods are not without their limitations, requiring skilled ultrasonographers and technical algorithms required to merge images (Franchi et al., 2019). The task specific skills for extended FOV collection including ultrasonography and technical skills (including coding ability) required as highlighted by Franchi et al (2019) does limit the useability of the extended FOV method in elite sport, as the time required will undoubtedly increase for both the practitioner and athlete. Time is a crucial component for elite training environments, with sport scientists being under constant pressure with strict time constraints especially within team-sport environments where large number of athletes would require assessing, which can impact upon method selection.

Significant differences have been found in PA measured from a single image compared to the extended FOV images (Pimenta et al., 2018), although this is not a consistent finding between studies (Franchi et al., 2019). These differences could explain why a single image would reduce the accuracy of any extrapolation method, particularly if it is attained from a short probe (6 cm). Furthermore, single image extrapolation methods demonstrate limited consistency and predictive ability to correct for errors (Franchi et al., 2019), this is consistent with the present study with both a negative and positive trend in bias, observed between the criterion method and basic trigonometry and partial measure methods, respectively (Figure 3). The comparison between criterion method and basic trigonometry estimations, demonstrated an enlarged bias for the shorter estimated FLs. In contrast however, the comparison between criterion method and partial measure methods revealed an elevated bias for the greater FLs. In conjunction with the results of the present study, these findings signify that the $BF_{LH}$ fascicles present significant complex curvature that could affect conclusions of ultrasound results when using different sonographic techniques (Franchi et al., 2019).

Although minimal differences between estimation methods were observed when using the current probe, the differences could be exacerbated when utilising a probe with a shorter FOV. Therefore, future research should aim to compare between the US procedures that have been utilised within the research, comparing between probe lengths on $BF_{LH}$ measurements (6 cm vs 10 cm). In addition, future research should look to determine sport specific univariate risk ratio (Timmins et al., 2016a; Dow et al., 2021), for variety of high-risk sports (e.g. European soccer, Gaelic football and rugby), where an elevated risk of HSI incidence is highlighted for a specific FL (Askling et al., 2003; Ekstrand et al., 2016; Opar et al., 2014; Orchard et al., 2017; Ruddy et al., 2018; Timmins et al., 2016a; Woods et al., 2004).

## Practical applications

Coaches, researchers and sport scientists, can use each of the extrapolation methods within the present study to identify meaningful changes in $BF_{LH}$ muscle architecture with very high inter session reliability along with SEM and MDD values provided for each of the estimation method. Additionally, any of the extrapolation methods used within the present study could be utilised to assess $BF_{LH}$ muscle architecture over time. Although only trivial differences identified between methods, with minimal mean bias (<5%); the 95% LOA were unacceptable (>5%) indicating that the methods could not be used or compared against. Furthermore, as the developed correction equations was not applicable it may not be appropriate to attempt to correct estimated FLs between methods. Although, extended FOV methods may be more accurate, it is still not considered the “gold standard” (Franchi et al., 2019), with several limitations including the time and skills required for collection and analysis of extended FOV imaging, Franchi et al., (2019) also highlights that there can be errors in the stitching between images via the texture mapping algorithms. However, very high repeatability can be observed for extended FOV methods (Pimenta et al., 2018; Franchi et al., 2019) and could therefore be a direction of future upskilling for practitioners. For practitioners working in elite team sport where time availability is limited, a single image extrapolation could be more feasible. Furthermore, as a key aim of HSI risk reduction training should be to lengthen the $BF_{LH}$ FL (Timmins et al., 2016a), it may be preferable for practitioners to retain underestimated results, ensuring a degree of cushioning when aiming for longer FL (i.e. estimated FL = 10.50 cm, actual FL = 10.80 cm).

**Declaration of interest Statement:** *The authors report there are no competing interests to declare.*

## References


Askling, C., Karlsson, J., & Thorstensson, A. (2003). Hamstring injury occurrence in elite soccer players after preseason strength training with eccentric overload. *Scandinavian Journal of Medicine and Science in Sports*, *13(4)*, 244-250. https://doi.org/10.1034/j.1600-0838.2003.00312.x

Behan, F. P., Vermeulen, R., Smith, T., Arnaiz, J., Whiteley, R., Timmins, R. G., & Opar, D. A. (2018). Poor agreement between ultrasound and inbuilt diffusion tensor MRI measures of biceps femoris long head fascicle length. *Translational Sports Medicine, 2(2),* 58-63. https://doi.org/10.1002/tsm2.58

Bland, J. M., & Altman, D. (1986). Statistical methods for assessing agreement between two methods of clinical measurement. *The lancet*, *327 (8476)*, 307-310. https://doi.org/10.1016/S0140-6736(86)90837-8

Blazevich, A. J., Gill, N. D., & Zhou, S. (2006). Intra- and intermuscular variation in human quadriceps femoris architecture assessed in vivo. *Journal of Anatomy*, *209*(3), 289-310. https://doi.org/10.1111/j.1469-7580.2006.00619.x

De Oliveira, V. B., Carneiro, S. P., & De Oliveira, L. F. (2016). Reliability of biceps femoris and semitendinosus muscle architecture measurements obtained with ultrasonography. *Revista Brasileira de Engenharia Biomedica, 32(4),* 365-371. https://doi.org/10.1590/2446-4740.04115

Dow CL, Timmins RG, Ruddy J, Williams MD, Maniar N, Hickey J., Bourne M.N., & Opar D.A. (2021). Prediction of Hamstring Injuries in Australian Football Using Biceps Femoris Architectural Risk Factors Derived From Soccer. *American Journal of Sports Medicine*, *49(13)*, *3687-3695*. https://doi.org/10.1177/03635465211041686

Ekstrand, J., Walden, M., & Hagglund, M. (2016). Hamstring injuries have increased by 4% annually in men's professional football, since 2001: a 13-year longitudinal analysis of the UEFA Elite Club injury study. *British Journal of Sports Medicine*, *50*(12), 731-737. https://doi.org/10.1136/bjsports-2015-095359

Franchi, M. V., Fitze, D. P., Raiteri, B. J., Hahn, D., & Spörri, J. (2019). Ultrasound-derived Biceps Femoris Long-Head Fascicle Length: Extrapolation Pitfalls. *Medicine &*

*Science in sports & Exercise*, *52(1), 233-243.* https://doi.org/10.1249/MSS.0000000000002123

Freitas, S.R., Marmeleira, J., Valamatos, J., Blazevich, A., & Mil-Homens, P. (2018). Ultrasonographic Measurement of the Biceps Femoris Long-Head Muscle Architecture. *Journal of Ultrasound in Medicine*, *37*(4), 977-986. https://doi.org/10.1002/jum.14436

Guilhem, G., Cornu, C., Guével, A., & Guevel, A. (2011). Muscle architecture and EMG activity changes during isotonic and isokinetic eccentric exercises. *European Journal of Applied Physiology*, *111(11)*, 2723-2733. https://doi.org/10.1007/s00421-011-1894-3

Hopkins, W. (2002). *A new view of statistics: A scale of magnitudes for effect statistics.* Sportscience.

Kawakami, Y., Abe, T., & Fukunaga, T. (1993). Muscle-fiber pennation angles are greater in hypertrophied than in normal muscles. *Journal of Applied Physiology*, *74(6)*, 2740-2744. https://doi.org/ 10.1152/jappl.1993.74.6.2740

Kellis, E., Galanis, N., Natsis, K., & Kapetanos, G. (2009). Validity of architectural properties of the hamstring muscles: correlation of ultrasound findings with cadaveric dissection. *Journal of Biomechanics*, *42*(15), 2549-2554. https://doi.org/10.1016/j.jbiomech.2009.07.011

Koulouris, G., & Connell, D. (2005). Hamstring Muscle Complex- An Imaging Review. *Radiographics*, *25*(3), 571-586. https://doi.org/10.1148/rg.253045711

Lieber, R. L., & Ward, S. R. (2011). Skeletal muscle design to meet functional demands. *Philosophical Transactions of the Royal Society London Series B, Biological Sciences*, *366*(1570), 1466-1476. https://doi.org/10.1098/rstb.2010.0316

Morin, J.B., Gimenez, P., Edouard, P., Arnal, P., Jimenez-Reyes, P., Samozino, P., Brughelli, M., & Mendiguchia, J. (2015). Sprint Acceleration Mechanics: The Major Role of Hamstrings in Horizontal Force Production. *Frontiers in Physiology*, *6*(404), 1-14. https://doi.org/10.3389/fphys.2015.00404

Opar, D.A., Drezner, J., Shield, A., Williams, M., Webner, D., Sennett, B., Kapur, R., Cohen, M., Ulager, J., Cafengiu, A., & Cronholm, P.F. (2014). Acute hamstring strain injury in track-and-field athletes: A 3-year observational study at the Penn Relay Carnival. *Scandinavian Journal of Medicine and Science in Sports*, *24*(4), e254-259. https://doi.org/10.1111/sms.12159

Opar, D.A., Williams, M., & Shield, A. (2012). Hamstring strain injuries: factors that lead to injury and re-injury. *Sports Medicine*, *42*(3), 209-226. https://doi.org/10.2165/11594800-000000000-00000

Orchard, J., Kountouris, A., & Sims, K. (2017). Risk factors for hamstring injuries in Australian male professional cricket players. *Journal of Sport and Health Science, 6*(3), 271-274. https://doi.org/10.1016/j.jshs.2017.05.004

Pimenta, R., Blazevich, A. J., & Freitas, S. R. (2018). Biceps Femoris Long-Head Architecture Assessed Using Different Sonographic Techniques. *Medicine and Science in Sports and Exerc*, *50*(12), 2584-2594. https://doi.org/10.1249/MSS.0000000000001731

Ribeiro Alvares, J. B., Dornelles, M. P., Fritsch, C. G., de Lima-e-Silva, F. X., Medeiros, T. M., Severo-Silveira, L., Marques, B., V., & Baroni, M. (2019). Prevalence of Hamstring Strain Injury Risk Factors in Professional and Under 20 Male Football (Soccer) Players. *Journal of Sport Rehabilitation*, 29(3), 339-345. https://doi.org/10.1123/jsr.2018-0084

Ruddy, J. D., Shield, A. J., Maniar, N., Williams, M. D., Duhig, S., Timmins, R. G., Hickey, J., Bourne, M. N., & Opar, D. A. (2018). Predictive Modeling of Hamstring Strain

Injuries in Elite Australian Footballers. *Medicine and Science in Sports Exercise*, *50*(5), 906-914. https://doi.org/10.1249/MSS.0000000000001527

Schache, A. G., Dorn, T. W., Wrigley, T. V., Brown, N. A., & Pandy, M. G. (2013). Stretch and activation of the human biarticular hamstrings across a range of running speeds. *European Journal of Applied Physiology*, *113*(11), 2813-2828. https://doi.org/10.1007/s00421-013-2713-9

Timmins, R. G., Bourne, M. N., Shield, A. J., Williams, M. D., Lorenzen, C., & Opar, D. A. (2016a). Short biceps femoris fascicles and eccentric knee flexor weakness increase the risk of hamstring injury in elite football (soccer): a prospective cohort study. *British Journal of Sports Medicine*, *50*(24), 1524-1535. https://doi.org/10.1136/bjsports-2015-095362

Timmins, R. G., Shield, A. J., Williams, M. D., Lorenzen, C., & Opar, D. A. (2015). Biceps femoris long head architecture: a reliability and retrospective injury study. *Medicine and Science in Sports and Exercise*, *47*(5), 905-913. https://doi.org/10.1249/MSS.0000000000000507

Timmins, R. G., Shield, A. J., Williams, M. D., Lorenzen, C., & Opar, D. A. (2016b). Architectural adaptations of muscle to training and injury: a narrative review outlining the contributions by fascicle length, pennation angle and muscle thickness. *British Journal of Sports Medicine, 50*(23), 1467-1472. https://doi.org/10.1136/bjsports-2015-094881

Woods, C., Hawkins, R. D., Maltby, S., Hulse, M., Thomas, A., Hodson, A., & Football Association Medical Research, P. (2004). The Football Association Medical Research Programme: an audit of injuries in professional football--analysis of hamstring injuries. *British Journal of Sports Medicine*, *38*(1), 36-41. https://doi.org/10.1136/bjsm.2002.002352

*Table 1 Between-session mean (SD), reliability and error statistics for bicep femoris long head architectural measurements.*

| | Muscle thickness (cm) | Pennation angle (°) | Criterion Measure (cm) | Basic Trigonometry (cm) | Partial Measure (cm) |
|---|---|---|---|---|---|
| **Mean (SD)** | 2.71 (0.02) | 16.11 (0.06) | 10.30 (0.03) | 9.97 (0.04) | 10.11 (0.03) |
| **CV (95% CI)** | 0.71 (0.70 - 0.72) | 0.35 (0.33 - 0.38) | 0.25 (0.24 - 0.26) | 0.37 (0.35 - 0.39) | 0.32 (0.31 - 0.34) |
| **ICC (95% CI)** | 0.972 (0.939 - 0.987) | 0.971 (0.937 - 0.995) | 0.989 (0.972 - 0.995) | 0.989 (0.975 - 0.995) | 0.998 (0.995 - 0.999) |
| ***p*** | 0.11 | 0.45 | 0.52 | 0.37 | 0.06 |
| ***g* (95% CI)** | 0.08 (-0.01 - 0.18) | 0.04 (-0.57 - 0.64) | 0.02 (-0.49 - 0.54) | 0.03 (-0.52 - 0.57) | 0.02 (-0.49 - 0.45) |
| **SEM** | 0.06 | 0.38 | 0.20 | 0.21 | 0.18 |
| **SEM%** | 2.17 | 2.36 | 1.93 | 2.11 | 1.78 |
| **MDD** | 0.16 | 1.06 | 0.55 | 0.58 | 0.50 |
| **MDD%** | 6.03 | 6.55 | 5.34 | 5.86 | 4.94 |

**Table 2. Bias and limits of agreement between the estimated measures of bicep femoris fascicle length**

| | | | 95% Limits of Agreement | | | |
|---|---|---|---|---|---|---|
| | | | **Lower** | **to** | **Upper** | **Ratio (SD)** |
| **Criterion vs. Basic Trigonometry** | **Bias** | 0.334 | -0.955 | - | 1.623 | 1.04 (0.05) |
| | **95% CI** | 0.069 to 0.600 | -1.415 to -0.495 | - | 1.163 to 2.083 | |
| | **Percent Bias (%)** | 3.24 | -9.27 | - | 15.76 | |
| **Criterion vs. Partial Measure** | **Bias** | 0.188 | -0.844 | - | 1.220 | 1.02 (0.04) |
| | **95% CI** | -0.025 to 0.401 | -1.213 to 0.476 | - | 0.852 to 1.589 | |
| | **Percent Bias (%)** | 1.83 | -9.19 | - | 11.84 | |

**Table 3. Observed relationships between the estimated measures of bicep femoris fascicle length**

| | Pearson's r (95% CI) | $R^2$ | *p* |
|---|---|---|---|
| **Criterion Vs Basic Trigonometry** | 0.945 (0.879 - 0.975) | 0.893 | < 0.001 |
| **Criterion Vs Partial Measure** | 0.961 (0.914 - 0.983) | 0.924 | < 0.001 |

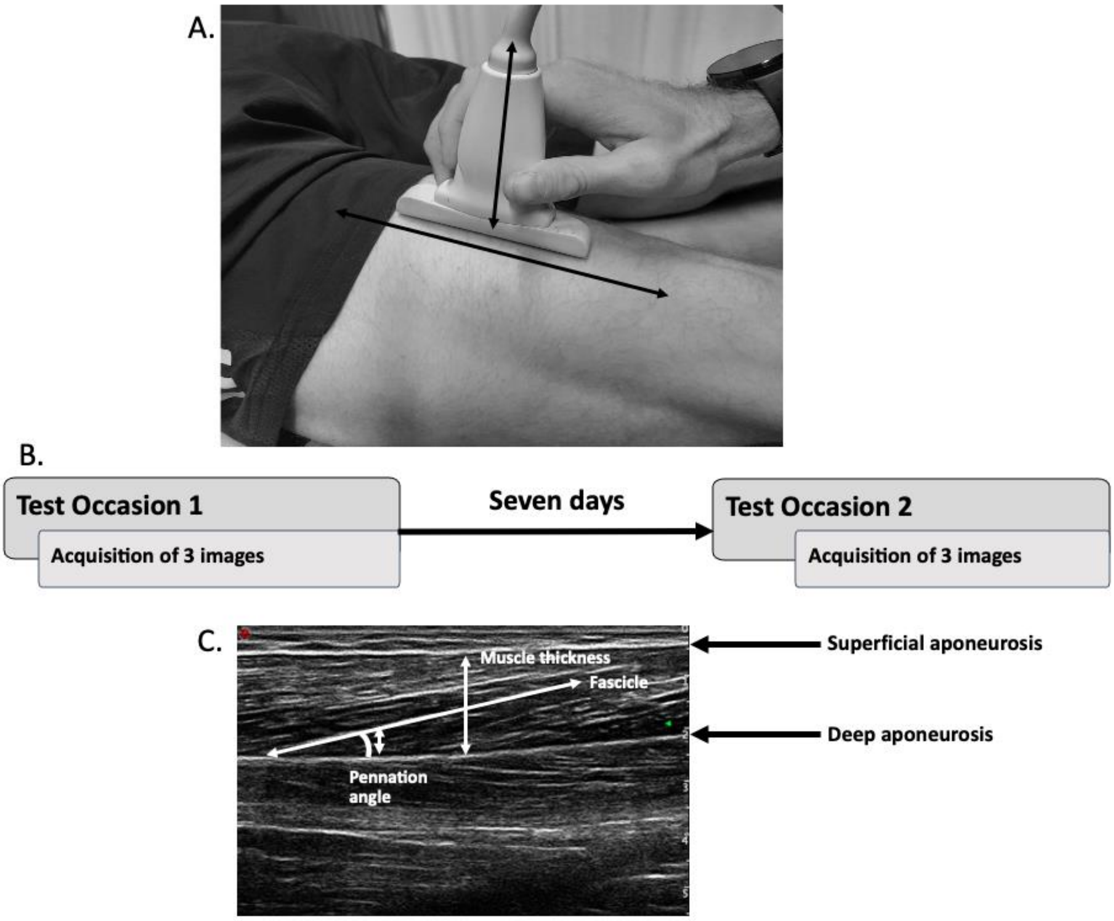


Figure 1. Experimental design and procedures used to assess bicep femoris long head fascicle length. A. Image acquisition using 10-cm ultrasound probe, with probe orientated perpendicular to the skin following the line of the bicep femoris (ischial tuberosity to lateral epicondyle). B. Experimental design with a timeline of test occasions and image acquisition. C. Example of sonogram image obtained of the bicep femoris with architectural features identified (muscle thickness, pennation angle, fascicle and aponeuroses (deep and superficial).

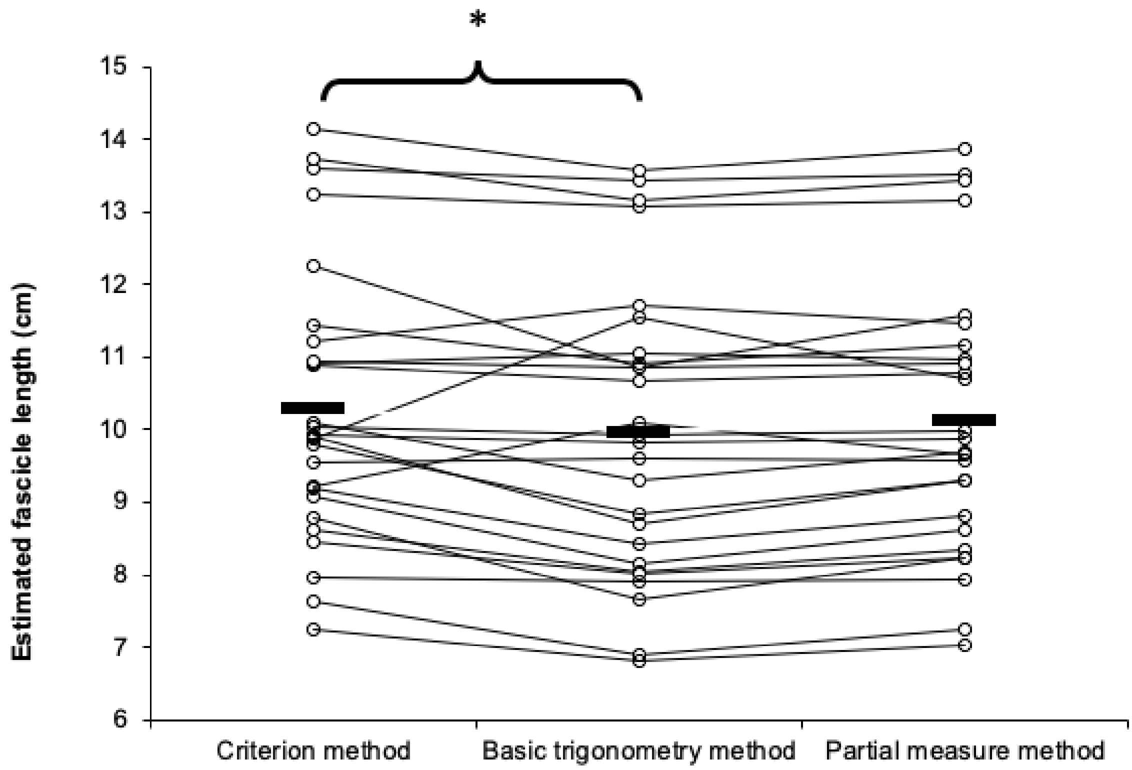


Figure 2. Differences in estimated fascicle length between the three methods of estimation, * = significant difference ($p < 0.05$). Black line signifying mean estimated fascicle length, where circles signify individual measurements.

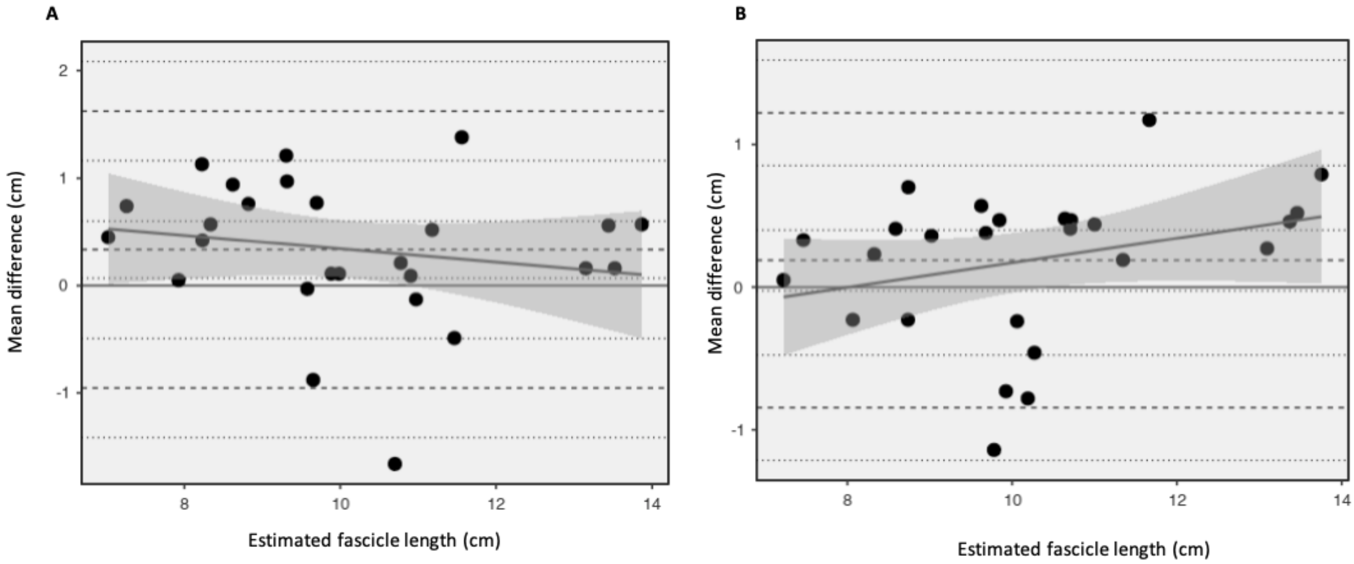


*Figure 3. Bland Altman plots comparing the mean estimated fascicle lengths between methods. A) criterion vs. basic trigonometry and B) criterion vs. partial measure methods.*

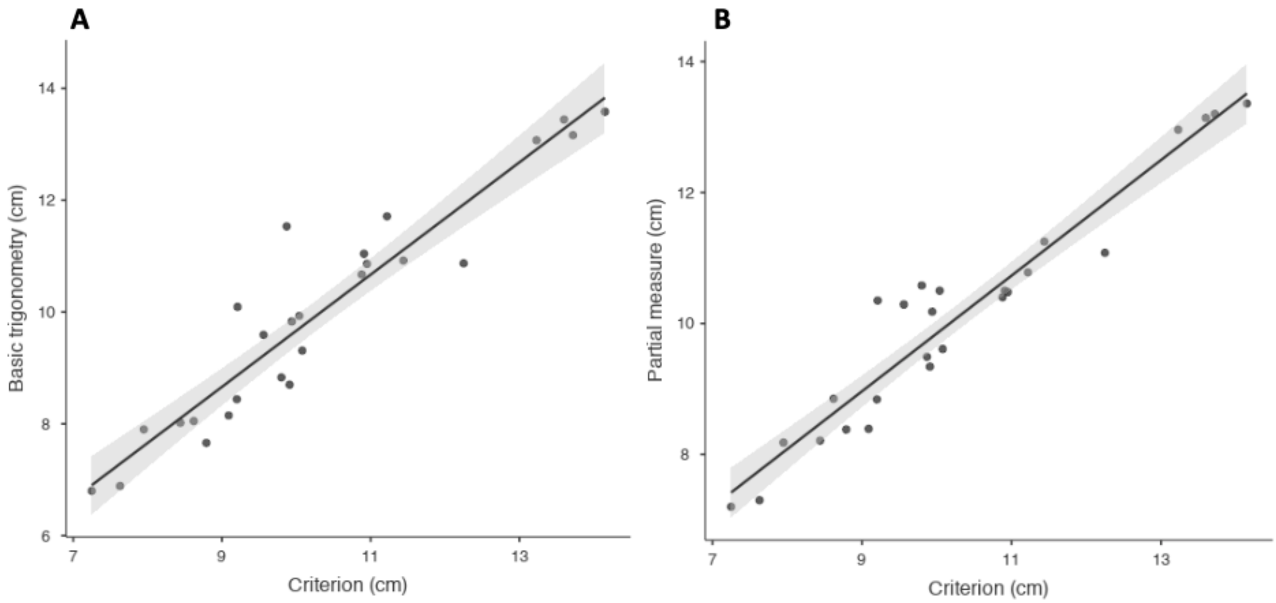


Figure 4. *Relationship and 95% confidence limits between the criterion and alternative methods of estimating bicep femoris long head fascicle length*